CHEMISTRY OF MATERIALS

Article

pubs.acs.org/cm

Phase Separation and Phase Transitions in Multiferroic $K_{0.58}FeF_3$ with the Tetragonal Tungsten Bronze Structure

Sandra A. Reisinger,[†] Marc Leblanc,[‡] Anne-Marie Mercier,[‡] Chiu C. Tang,[§] Julia E. Parker,[§] Finlay D. Morrison,[†] and Philip Lightfoot*,[†]

[†]School of Chemistry and EaStChem, University of St. Andrews, St. Andrews, Fife, KY16 9ST, United Kingdom

[‡]Laboratoire des Oxydes et Fluorures, Faculté des Sciences et Techniques, Université du Maine, 72085, Le Mans Cedex 9, France

[§]Diamond Light Source Ltd., Harwell Science and Innovation Campus, Didcot, Oxfordshire, OX11 0DE, United Kingdom

Supporting Information

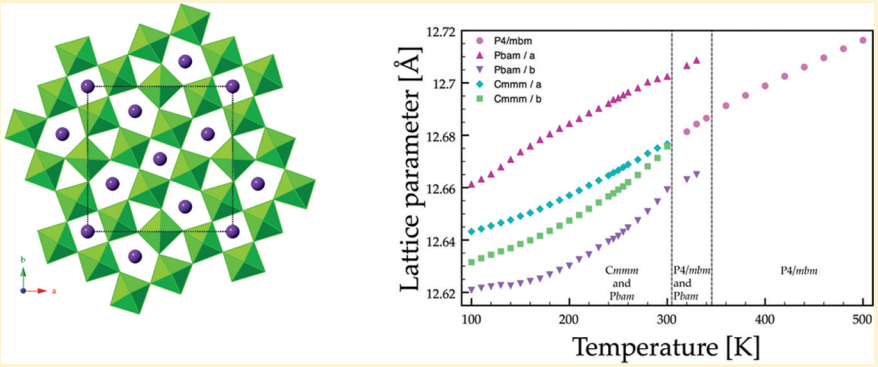

ABSTRACT: The tetragonal tungsten bronze (TTB) structure multiferroic fluoride $K_{0.58}FeF_3$ (alternatively $K_{3-x}Fe_5F_{15}$ ($x \approx 0.1$)) has been studied using variable temperature high-resolution synchrotron powder X-ray diffraction. The as-made sample occurs as a mixture of two closely related TTB phases, one tetragonal ($a_{TTB} \approx 12.68$ Å, $c_{TTB} \approx 3.98$ Å) and one orthorhombic ($a \approx 12.70$ Å, $b \approx 12.66$ Å, $c \approx 3.98$ Å). Heating above 340 K produces a single metrically tetragonal phase, but the phase separation reproducibly reappears on cooling. Below 300 K the tetragonal phase undergoes a structural phase transition to a second orthorhombic phase (with $a \approx b \approx \sqrt{2}\, a_{TTB}$) and these two different orthorhombic phases continue to coexist down to at least 125 K. These results are discussed in the context of previous studies, which sometimes suggest conflicting structural details within this system.

KEYWORDS: *tetragonal tungsten bronze structure, phase transition, phase separation, multiferroic*

INTRODUCTION

During the recent resurgence of interest in the field of multiferroics, the vast majority of candidate materials studied have been oxides.[1−3] However, there is no intrinsic reason why simultaneous ferroelectric, ferroelastic and/or magnetic ordering cannot be found in other systems, for example fluorides.[4,5] $K_{3-x}Fe_5F_{15}$ represents probably the most studied fluoride-based multiferroic material to date, and is interesting for a number of reasons. Early work[6] showed that a phase of composition $K_3Fe_5F_{15}$ (alternatively formulated as $K_{0.6}Fe^{II}_{0.6}Fe^{III}_{0.4}F_3$) crystallized in the tetragonal tungsten bronze (TTB) structure type (Figure 1), with a polar orthorhombic distortion (space group *Pba*2, $a \approx 12.75$ Å, $b \approx 12.64$ Å, $c \approx 3.99$ Å) of the aristotype tetragonal phase ($a = a_{TTB} \approx 12.7$ Å, $c = c_{TTB} \approx 3.99$ Å; space group *P*4/*mbm*)[7] at room temperature. Bond distances around the three distinct Fe sites suggested a partial ordering of Fe^{II}/Fe^{III}. The small polar deviation from the parent symmetry also suggested the possibility of both ferroelectric and ferroelastic behavior, and this was later confirmed experimentally by Ravez et al.[8] These researchers proposed a simultaneous, coupled ferroelectric/ferroelastic transition at 490 K, on the basis of dielectric, calorimetric, resistivity and optical measurements, and suggested that Fe^{II}/Fe^{III} disordering might be concomitant, with a change of point group from *mm*2 to 4/*mmm*. The charge-disordering was later confirmed by Mossbauer spectroscopy.[9] A follow-up investigation looked at the off-stoichiometric variants $K_{3-x}Fe_5F_{15}$ ($0 < x < 0.20$) and reported a remarkable sensitivity of both crystallographic symmetry and ferroelectric properties versus composition, the samples becoming tetragonal at room temperature for $x > 0.075$, and T_C falling to 230 K for $x = 0.20$, compared to $T_C = 490$ K for $x = 0$.[10]

A later study by Ishihara et al.,[11] identified two further phase transitions, one around 120 K being of magnetic origin, and

Received: September 12, 2011
Revised: November 14, 2011
Published: November 15, 2011

 © 2011 American Chemical Society

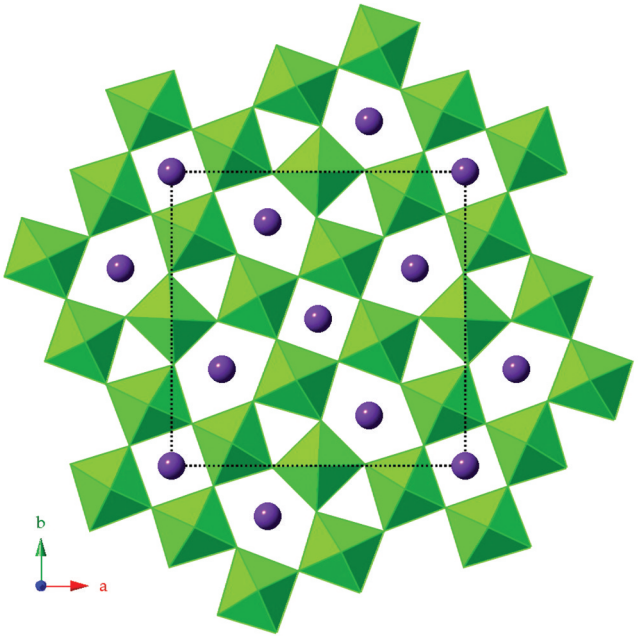

Figure 1. Aristotype TTB structure.

one around 290 K being a structural phase transition observed optically by the formation of different ferroelastic domain patterns. This was ascribed to the growth of a low temperature monoclinic phase within the existing orthorhombic phase. More detailed crystallographic studies have been undertaken recently by Calestani and colleagues. First, for a composition $K_{0.53}FeF_3$ a complex orthorhombic supercell of the aristotype TTB with $a' \sim 2\sqrt{2}\ a_{TTB}$, $b' \sim \sqrt{2}\ b_{TTB}$, $c' \sim 2\ c_{TTB}$ was observed at room temperature using a combination of electron diffraction and single crystal X-ray diffraction.[12] This distortion was ascribed to a combination of charge-ordering (CO) and ferroelectric (FE) symmetry-lowerings, with the latter being related to an 'octahedral-tilt' mode. Second, a composition close to $K_{0.59}FeF_3$ was studied,[13] and found to exhibit the (CO) superstructure but not the octahedral tilt superstructure at room temperature (note here that the (CO) superstructure gives rise to the $c' = 2\ c_{TTB}$ cell axis, implying charge-ordering in alternating sites along the *c*-axis, in contrast to the early model of Hardy et al.[6]). However, the octahedral tilt (FE) superstructure was found to grow in on decreasing the temperature below about 290 K. The unit cell of the resulting commensurate superlattice was then suggested to be monoclinic, with $a' \approx 2\sqrt{2}\ a_{TTB}$, $b' \approx 2\ c_{TTB}$, $c' \approx \sqrt{2}\ b_{TTB}$, $\beta \approx 90.4°$. This suggestion appears to support the earlier optical study of Ishihara et al.[11] Furthermore, on heating, these authors concluded that the orthorhombic − tetragonal transition for the basic subcell did not occur until around 570 K, i.e. 80 K above the previously reported ferroelectric/ferroelastic transition. The most recent study by these authors,[14] of a composition near $K_{0.6}FeF_3$, carries out detailed magnetization measurements on single-crystal samples, together with a determination of the magnetic structure by powder neutron diffraction, and concludes a ferrimagnetic structure below 116 K with considerable frustration and anisotropy. Both the magnetic and crystal structure are modeled with an approximate unit cell the size of the (CO) superstructure described above (nuclear space group *Pba*2, $a \approx b \approx a_{TTB}$, $c \approx 2c_{TTB}$).

In the light of these results, there are clearly some remaining ambiguities in the phase diagram of $K_{3-x}Fe_5F_{15}$, and the present work aims to clarify some of these issues by carrying out a careful structural study of $K_{3-x}Fe_5F_{15}$ using high-resolution synchrotron powder X-ray diffraction over a wide temperature range (100−500 K), including all the potential phase transitions. For a composition around $x \approx 0.10$ (i.e., $K_{2.9}Fe_5F_{15}$ or alternatively $K_{0.58}FeF_3$) our study produced a somewhat unexpected result: a phase separation, rather than simply discrete phase transitions, which adds further complexity to this extraordinary system.

EXPERIMENTAL SECTION

Synthesis. KF (10 mmol, 0.58 g), FeF_2 (6.4 mmol, 0.60 g), and FeF_3 (3.6 mmol, 0.41 g) were mixed in a glovebox under a dry nitrogen atmosphere and placed in a Pt tube. The tube was dehydrated and degassed at 120 °C overnight, then sealed and heated to 710 °C for 48 h.

Powder X-ray Diffraction (PXRD). Preliminary analysis of sample quality was carried out in-house using a Stoe STADI/P diffractometer ($CuK_{\alpha 1}$ radiation). Variable-temperature studies were performed at beamline I11 at Diamond Light Source, UK[15] at a wavelength of 0.825558(2) Å. On this instrument 45 individual detectors are used to collect data simultaneously over the full 2θ range, with only a 30° scan. Data are collected at a nominal resolution of 0.8 mdeg, but then normalized and rebinned into constant 1 mdeg steps. Diffraction patterns were collected at 34 temperatures between 100 and 500 K, the temperature was controlled using an Oxford Cryostream Plus system. Each pattern was collected for 30 min. The as-made sample was first studied at ambient temperature, followed by warming to 500 K and subsequently cooling to 100 K. A series of additional diffraction patterns were measured on thermal cycling of samples in the region 300−360 K. Samples were mounted in 0.5 mm glass capillaries. Rietveld refinements were carried out using the GSAS package.[16]

RESULTS

As will be seen later, the as-made sample consists of a mixture of two different TTB-like phases. For reasons of clarity, we therefore present the results of the higher-temperature data collections first, so that the phase evolution can be understood in a more natural way.

Parent Phase at 500 K. As reported in the Introduction, there are conflicting reports as to the crystal system of the potassium-rich end of the solid solution (i.e., near $K_{0.6}FeF_3$) above 490 K. Both orthorhombic and tetragonal phases have been suggested, although full structural models have not been reported at this temperature. There are three issues to determine concerning the structure above 490 K: (i) is the crystal system metrically tetragonal, as suggested by the optical studies of Ravez et al.,[8] or orthorhombic, as suggested by the PXRD of Mezzadri et al.?[13] (ii) is the *c*-axis doubled? (iii) is it possible to distinguish between centrosymmetric and polar models? To probe these questions, both an orthorhombic model (*Pba*2; $a \approx b \approx a_{TTB}$, $c = 2c_{TTB}$)[13] and the (CO) tetragonal model ($P4_2bc$; $a = b = a_{TTB}$, $c = 2c_{TTB}$)[12] were fitted to the data at 500 K. No evidence of an orthorhombic distortion is found; the lattice parameters refine to be exactly equal ($a = b = 12.7160(3)$ Å). Moreover, the as-input model gives a higher R-factor than the much simpler *P*4/*mbm* model eventually chosen, and all attempts to refine the orthorhombic model led to instabilities and no significant improvement in fit. We conclude that the phase is metrically, and probably also crystallographically, tetragonal at this temperature.

dx.doi.org/10.1021/cm202713n | *Chem. Mater.* 2011, 23, 5440−5445

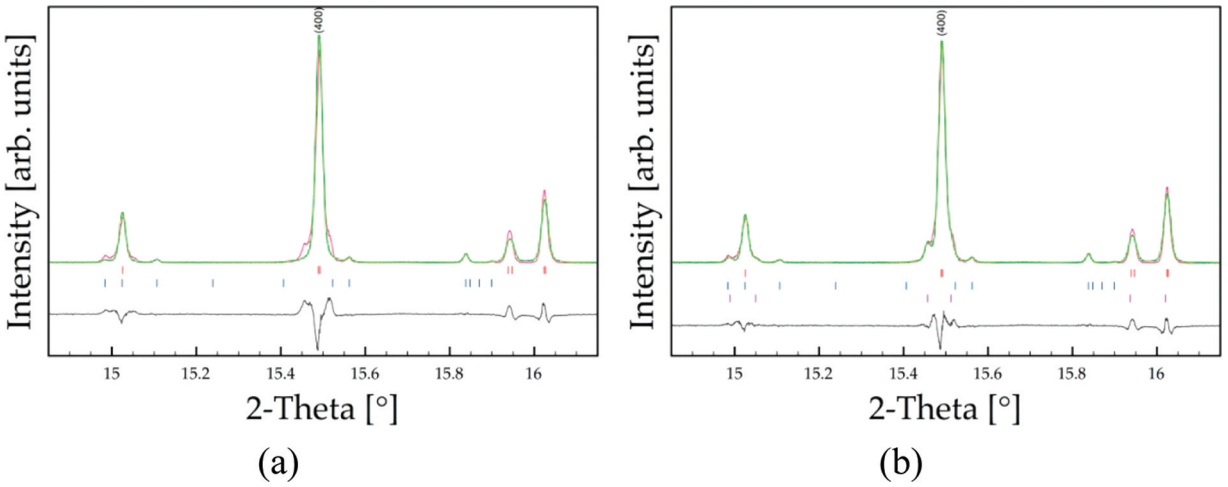

Figure 2. Shoulders on the (400) peak at 320 K modeled using (a) only the *P*4/*mbm* model and (b) the *P*4/*mbm* and *Pbam* models.

A further comparison of three tetragonal models was then made to determine if there is any evidence for both *c*-axis doubling or lowering of symmetry to a polar phase. The tetragonal models used were the aristotype TTB model (*P*4/*mbm*; $a = a_{TTB}$, $c = c_{TTB}$), the (CO) tetragonal model and the polar model (P4*bm*; $a = a_{TTB}$, $c = c_{TTB}$). Doubling the *c*-axis allows indexing and fitting of only one additional very weak reflection near 9.5° (indexed as 201 in the doubled cell; see the Supporting Information). However, once again the as-input model produced a higher R-factor than the *P*4/*mbm* model, and attempts at refinement of atomic parameters led to instabilities. Lowering of the symmetry to *P*4*bm* also allows only a very marginal improvement in fit (R_{wp} = 11.88% versus 11.95% for the *P*4/*mbm* model) for the additional 8 refineable atomic coordinates. We therefore conclude that the structure is centrosymmetric and tetragonal at 500 K, within the limitations of this experiment; although there is very weak evidence for a doubled *c*-axis, it is not possible to identify the origin of this from the data we have, and an approximate model in P4/*mbm* ($a = a_{TTB}$, $c = c_{TTB}$) is used. Refinement of the occupancies of the two distinct K sites related that K(1) was fully occupied, whereas K(2) refined to about 90% occupancy, thus supporting the assignment of the composition as $K_{0.58}FeF_3$. Further details of these models are provided in the Supporting Information.

Analysis of the bond lengths surrounding the two Fe sites within the unit cell, indicate that the Fe2 (8j) site is preferred for Fe^{2+} and the Fe1 (2c) site is preferred by Fe^{3+}. The Fe2 site is the one that makes up the "perovskite-like" core of the structure. Bond lengths average 2.01 Å and 1.99 Å for the two sites respectively. The bond valence sums for the two sites, calculated from the data presented by Brese and O-Keefe,[17] are 2.62 (Fe1) 2.26 (Fe2). Thus, it seems that this model is charge-ordered, in the same sense as originally suggested by Hardy.[6]

Traces of two impurity phases, K_2FeF_5 and α-Fe_2O_3, are present in all the data sets. They are well characterized over the entire temperature range and represent around 3 and 1.6% by weight, respectively; further details are given in the Supporting Information. Significant evidence of preferred orientation for the TTB phase is also found, and this has been corrected for using a spherical harmonics model.[18]

Phase Evolution 500−300 K. The aristotype *P*4/*mbm* model gives a similar level of fit throughout the range 500−340 K. Below 340 K shoulders appear on the (*h*00/0*k*0) peaks of the TTB phase (Figure 2). This suggests a phase separation into two very similar TTB phases, with the emergent phase exhibiting a nonequivalence of the *a* and *b* lattice parameters. The shoulders are well indexed by an orthorhombic model (Figure 2) using the space group *Pbam* ($a \approx b \approx a_{TTB}$, $c = c_{TTB}$). This model is the simplest lower symmetry subgroup of the original *P*4/*mbm*. We stress that this is an approximate model only; the orthorhombic distortion is unambiguous and there is no evidence for an increase in unit cell volume, or additional superlattice, e.g., of the (FES) type, but we cannot rule out a more subtle distortion, for example to the polar space group *Pba*2, previously observed at room temperature. A structural model for the "*Pbam*" phase was generated using ISODISTORT[19] and a four-phase refinement (i.e., including the two coexisting TTB phases) was carried out at 320 K and several temperatures below this. Because of the severe peak overlap between the two TTB phases, it was not sensible to refine the internal structure of either phase at temperatures below 340 K, but lattice parameters and phase fractions were refined, leading to stable refinements and well-defined results. Example unit-cell data for this two-TTB-phase model are given in Table 1.

Table 1. Crystal Data for the Two Phases of $K_{0.58}FeF_3$ at 320 K (χ^2 = 2.126, wR_p = 18.83%, R_p = 14.51%)

space group	*P*4/*mbm*	*Pbam*
cryst syst	tetragonal	orthorhombic
unit-cell dimensions (Å)	a = 12.68136(2)	a = 12.7066
	c = 3.977009(8)	b = 12.6631
		c = 3.9780
volume (Å^3)	639.570(3)	640.084
Z	2	2

The *Pbam* phase grows in rapidly from 0% at 340 K to around 10% at 300 K and remains approximately constant below this (see the Supporting Information). The *a* and *b* lattice parameters of this phase are significantly different to each other on its first appearance at 320 K, suggesting a first-order phase transition of part of the sample. The *c* lattice parameter, conversely, is very similar to the tetragonal one (Figure 3). Below 300 K, a further event occurs, which can be ascribed to a structural phase transition of the tetragonal TTB phase.

dx.doi.org/10.1021/cm202713n | *Chem. Mater.* 2011, 23, 5440−5445

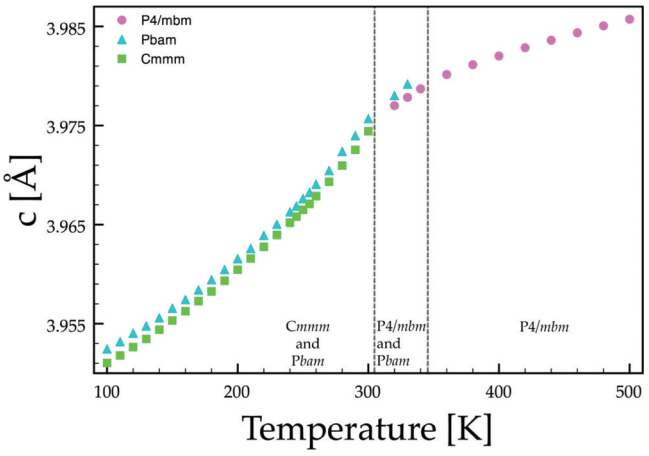

Figure 3. Lattice parameter *c* as a function of temperature.

Phase Evolution below 300 K. Below 300 K, the (*hh*0) peaks in the tetragonal model broaden and eventually split (Figure 4). An analysis of the full-width-at-half-maximum (fwhm) of these peaks, compared to a reference peak, indicates a lowering of symmetry commencing around 300 K (see the Supporting Information) and at 100 K two distinct peaks are clearly visible. This type of splitting can be explained by a monoclinic distortion of the primitive subcell (i.e., $a = b = a_{TTB}$, $\beta \neq 90°$, without a change in unit cell volume), rather than a divergence of the a and b parameters, as described above. More conventionally, the supercell is described as orthorhombic but with a doubling of unit cell volume (i.e., $a' \approx \sqrt{2}\, a_{TTB}$, $b' \approx \sqrt{2}\, a_{TTB}$, $c' \approx c_{TTB}$). This naturally leads to a C-centered supercell, which has previously been reported in several oxide TTBs.[20,21] The simplest model for this second orthorhombic phase can be described in space group *Cmmm* (Figure 5). Again, we stress

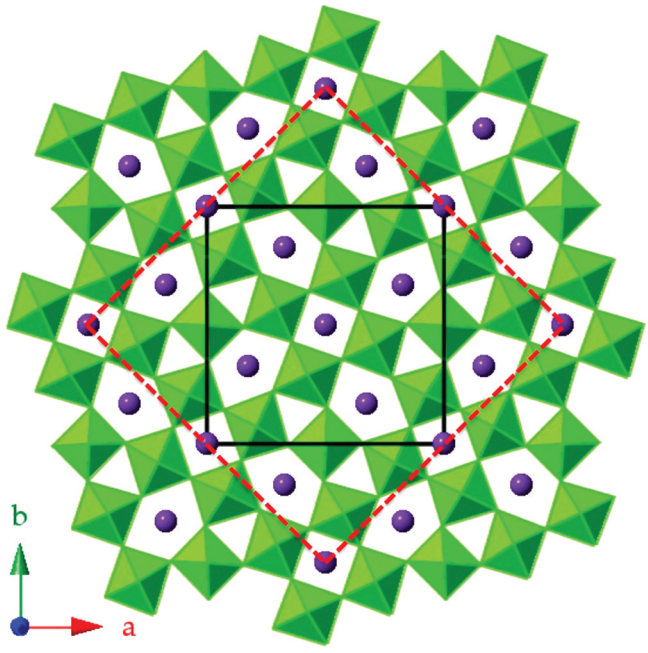

Figure 5. The unit cells of the *P*4/*mbm* and *Pbam* models (black, solid line) and the *Cmmm* model (red, dashed line).

that this is certainly an approximation, and the true symmetry is probably lower (at least a polar subgroup and possibly a further supercell of the (FES) type, although we see no additional superlattice peaks). An idealized *Cmmm* model was therefore derived using ISODISTORT and a second two-TTB-phase refinement (i.e., *Pbam* + *Cmmm*) was used for all the lower-temperature data sets. Once again, the internal structures of these models were not refined, but robust and reliable phase fractions and lattice parameters were obtained; an example is

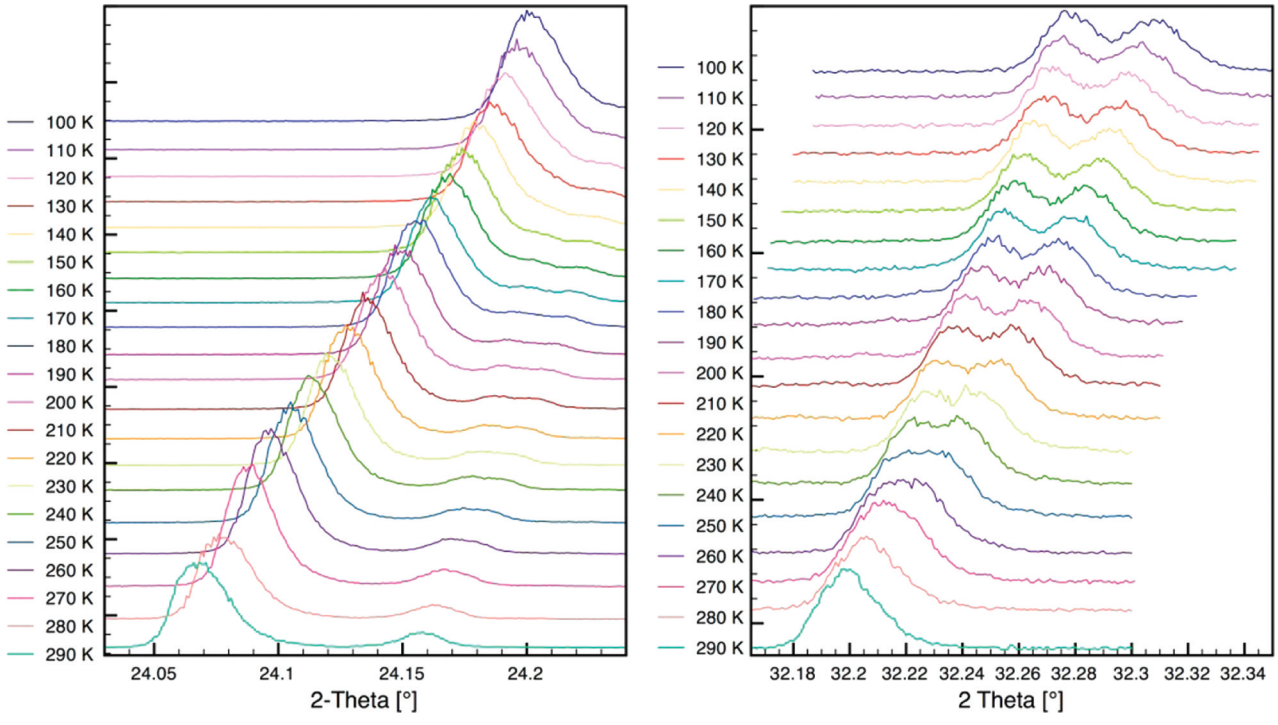

Figure 4. Excerpts from the PXRD patterns of $K_{0.58}FeF_3$ as a function of temperature indicating the constant nature of the (002) reference peak on the left, and the splitting of the "(660)" peak of the tetragonal model on the right.

dx.doi.org/10.1021/cm202713n | *Chem. Mater.* 2011, 23, 5440–5445

given in Table 2. The orthorhombic distortion of the *Cmmm* phase is much more subtle than that of the *Pbam* phase, and the phase transition appears to be continuous, with a and b converging near 300 K. Both these features can be seen in a combined plot of all the lattice parameters for the three TTB phase fields as a function of temperature (Figure 6). Note that the orthorhombic distortion of the *Cmmm* phase continues to increase toward lower temperatures whereas the *Pbam* phase shows more complex behavior. The refinements are robust and "well-behaved"' with the caveat that only approximations to the true internal structural distortions are assumed.

Table 2. Crystal Data for the Two Phases of $K_{0.58}FeF_3$ at 270 K (χ^2 = 1.687, wR_p = 15.80%, R_p = 12.26%)

space group	*Pbam*	*Cmmm*
cryst syst	orthorhombic	orthorhombic
unit-cell dimensions (Å)	a = 12.69810(5)	a = 17.91907(4)
	b = 12.64743(6)	b = 17.91082(5)
	c = 3.97045(2)	c = 3.969330(7)
V (Å^3)	637.648(4)	1273.570(3)
Z	2	4

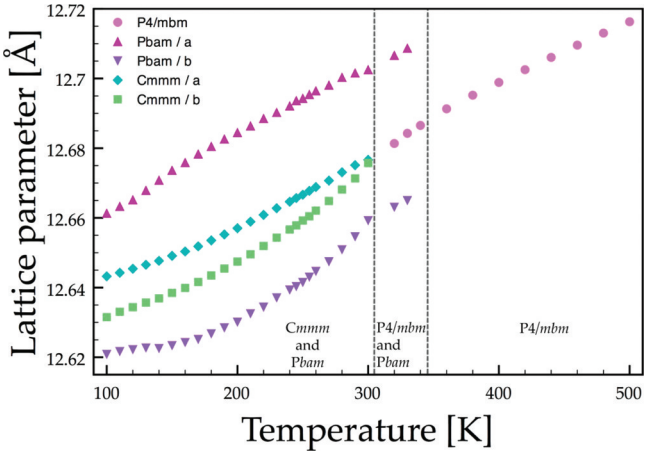

Figure 6. Lattice parameters a and b as a function of temperature (those for the *Cmmm* model are divided by $\sqrt{2}$ to allow direct comparison).

A further subtlety is seen at temperatures close to 100 K. The extremely high resolution of the powder diffractometer (beamline I11) reveals tentative evidence that the *Cmmm* phase may have a weak incommensurate distortion. For example, the (12,0,0) and (0,12,0) peaks are shifted, albeit by less than 0.01°, compared to standard (hkl) peaks in the same phase (see the Supporting Information). This shift in (h00/0k0) peaks may be caused by an incommensurate distortion in the *ab* plane. Several oxide-based TTB compounds, in particular the solid solutions of sodium barium niobate $Ba_2Na_{1-x}Nb_5O_{15}$,[22] also show an incommensurate distortion of a similar type at low temperatures. The distortions in these other TTBs are attributed to octahedral tilting and dipolar order.[23,24]

Discussion and Conclusions. The as-made sample of $K_{0.58}FeF_3$, at ambient temperature, exists as a mixture of two distinct TTB phases, designated herein as *P*4/*mbm* and *Pbam*. On warming to 500 K, the phases merge to a single metrically tetragonal phase. On subsequent cooling the phase separation reappears at around 340 K, followed by a further phase transition of the majority tetragonal phase around 300 K. Subsequent in situ heating/cooling cycles were carried out on different samples in order to establish the reproducibility of the phase separation: heating the samples above 360 K (i.e., into the single tetragonal phase field) and then cooling at varying rates to 300 K shows that the ratio of the two phases coexisting below 340 K remains essentially unchanged. The phase separation is therefore a thermodynamic rather than a kinetic phenomenon, and presumably relates to a miscibility gap in the solid solution as a function of the potassium content, x. The *P*4/*mbm* and *Pbam* phases are suggested most likely to differ fundamentally in potassium content (and therefore probably also Fe^{2+}/Fe^{3+} ratio), and this may subsequently drive their differing crystallographic distortions and the lower temperature phase transition. It is not possible to determine, from the present data, whether the differing structural distortions are due to charge ordering, octahedral tilting, polar atomic displacements or some other mechanism. Nevertheless, our observation of the consecutive appearance of two distinct orthorhombic phases on cooling the sample from the parent tetragonal phase is unambiguous. So too, is the coexistence of two different TTB phases in the regions 340−300 K and 300−100 K. This may have important consequences for the interpretation of the physical properties of materials in this system; for example the two phases will likely have differing ferroelectric and magnetic ordering behavior, both in terms of the temperatures of ordering and also their nature. It is likely that the phase transition we observe around 300 K is a related phenomenon to that reported by Ishihara et al.,[11] although they suggest a monoclinic phase (a possible alternative description of our *Cmmm* phase) growing into an already orthorhombic phase, with no evidence of a simultaneous tetragonal phase.

This work exploits the advantages of powder diffraction, and in particular the supreme resolution of a synchrotron-based experiment, to shed further insight into the complex phase behavior of this family of multiferroic fluorides. The key advantage of powder diffraction over single-crystal methods or electron diffraction is that the bulk sample is studied simultaneously, rather than a single and possibly unrepresentative crystal or grain. Phase separation phenomena, phase coexistence, and the evolution of phases across phase transitions are therefore much easier to identify and more reliably and unambiguously modeled across the whole sample. The natural disadvantage is that the peak overlap inherent in the method, even at very high resolution, necessitates the approximations referred to above and ultimately prohibits the exact, underlying structural mechanisms for the observed phase behavior from being established.

A multipronged approach, including each of these methods is therefore optimal to provide a fuller picture of the complex phase behavior in this and related systems. The very subtle (FES) superstructure reported by Calestani and co-workers[12,13] was principally identified by electron diffraction, although the details could subsequently be verified by single-crystal XRD. In fact, our own simulations of synchrotron powder XRD, at the resolution of the present experiment, based on the Calestani models show that we could not expect to see any evidence of the larger supercell or the further monoclinic distortion previously suggested; the additional features are too weak. High-resolution neutron powder diffraction data might be desirable in this respect. More detailed physical property measurements are also required, especially in the light of the

dx.doi.org/10.1021/cm202713n | *Chem. Mater.* 2011, 23, 5440−5445

phase separations reported here. It is very difficult to tell whether any of the phases proposed here, even the single tetragonal phase at 500 K, are centrosymmetric or not directly from the diffraction data: confirmatory dielectric measurements would be required.

The experimental studies, together with various insights and hints from previous work, suggest that there are several competing mechanisms of structural distortion inherent in this system. In fact, a recent computational DFT study[25] suggests there are a number of different charge-ordered models of similar energy, which can give drive distortions to ferroelectric states with differing polarization directions and magnitudes. In addition to the specific new insights identified above, the underlying message from the present study is that care must be taken in correlating the physical properties of these complex multiferroic materials with structural information obtained from an incomplete suite of techniques. Each technique has its contribution to make, but omitting one may lead to ambiguities, artifacts, or false interpretations.

■ ASSOCIATED CONTENT

Supporting Information

Further details of Rietveld refinements, structural models, and Rietveld plots. This material is available free of charge via the Internet at http://pubs.acs.org.

■ AUTHOR INFORMATION

Corresponding Author

*E-mail: pl@st-and.ac.uk.

■ ACKNOWLEDGMENTS

We would like to thank EPSRC for funding. This work was carried out with the support of Diamond Light Source. F.D.M. thanks the Royal Society for a Research Fellowship. The University of St. Andrews is thanked for partial support of a studentship to S.A.R..

■ REFERENCES

(1) Cheong, S.-W.; Mostovoy, M. *Nat. Mater.* **2007**, *6*, 13−20.
(2) Fiebig, M. *J. Phys. D: Appl. Phys.* **2005**, *38*, R123.
(3) Kimura, T.; Goto, T.; Shintani, H.; Ishizaka, K.; Arima, T.; Tokura, Y. *Nature* **2003**, *426*, 55−58.
(4) Nenert, G.; Palstra, T. T. M. *J. Phys.: Condens. Matter* **2007**, *19*, 406213.
(5) Scott, J. F.; Blinc, R. *J. Phys.: Condens. Matter* **2011**, *23*, 113202.
(6) Hardy, A. M.; Hardy, A.; Ferey, G. *Acta Crystallogr., Sect. B* **1973**, *29*, 1654−1658.
(7) Magneli, A. *Ark. Kemi* **1949**, *1*, 213−221.
(8) Ravez, J.; Abrahams, S. C.; de Pape, R. *J. Appl. Phys.* **1989**, *65*, 3987−3990.
(9) Calage, Y.; Abrahams, S. C.; Ravez, J.; de Pape, R. *J. Appl. Phys.* **1990**, *67*, 430−433.
(10) Ravez, J.; Abrahams, S. C.; Mercier, A. M.; Rabardel, L.; de Pape, R. *J. Appl. Phys.* **1990**, *67*, 2681−2683.
(11) Ishihara, S.; Rivera, J. P.; Kita, E.; Ye, Z. G.; Kubel, F.; Schmid, H. *Ferroelectrics* **1994**, *162*, 399−409.
(12) Fabbrici, S.; Montanari, E.; Righi, L.; Calestani, G.; Migliori, A. *Chem. Mater.* **2004**, *16*, 3007−3019.
(13) Mezzadri, F.; Fabbrici, S.; Montanari, E.; Righi, L.; Calestani, G.; Gilioli, E.; Bolzoni, F.; Migliori, A. *Phys. Rev. B: Condens. Matter* **2008**, *78*, 064111.
(14) Mezzadri, F.; Calestani, G.; Pernechele, C.; Solzi, M.; Spina, G.; Cianchi, L.; Del Giallo, F.; Lantieri, M.; Buzzi, M.; Gilioli, E. *Phys. Rev. B: Condens. Matter* **2011**, *84*, 104418.
(15) Thompson, S. P.; Parker, J. E.; Potter, J.; Hill, T. P.; Birt, A.; Cobb, T. M.; Yuan, F.; Tang, C. C. *Rev. Sci. Instrum.* **2009**, *80*, 075107−075109.
(16) Larson, A. C.; R. B. von Dreele. *General Structure Analysis System GSAS*; Report LAUR-86-748 ; Los Alamos National Laboratory: Los Alamos, NM, 1987.
(17) Brese, N. E.; O'Keeffe, M. *Acta Crystallogr., Sect. B* **1991**, *47*, 192−197.
(18) Von Dreele, R. B. *J. Appl. Crystallogr.* **1997**, *30*, 517−525.
(19) Campbell, B. J.; Stokes, H. T.; Tanner, D. E.; Hatch, D. M. *J. Appl. Crystallogr.* **2006**, *39*, 607−614.
(20) Chi, E. O.; Gandini, A.; Min, O. K.; Lei, Z.; Halasyamani, P. S. *Chem. Mater.* **2004**, *16*, 3616−3622.
(21) Labbe, P. H.; Frey, M.; Allais, G. *Acta Crystallogr., Sect. B* **1973**, *29*, 2204−2210.
(22) Filipic, C.; Kutnjak, Z.; Lortz, R.; Torres-Pardo, A.; Dawber, M.; Scott, J. F. *J. Phys.: Condens. Matter* **2007**, *19*, 236206.
(23) Levin, I.; Stennett, M. C.; Miles, G. C.; Woodward, D. I.; West, A. R.; Reaney, I. M. *Appl. Phys. Lett.* **2006**, *89*, 122908.
(24) Schneck, J.; Toledano, J. C.; Joffrin, C.; Aubree, J.; Joukoff, B.; Gabelotaud, A. *Phys. Rev. B: Condens. Matter* **1982**, *25*, 1766.
(25) Yamauchi, K.; Picozzi, S. *Phys. Rev. Lett.* **2010**, *105*, 107202.